ACS APPLIED MATERIALS & INTERFACES

www.acsami.org

Research Article

Facile Preparation of Dual Functional Wearable Devices Based on Hindered Urea Bond-Integrated Reprocessable Polyurea and AgNWs

Xingyuan Lu, Lun Zhang, Jihai Zhang, Chao Wang, and Aimin Zhang*

Cite This: https://doi.org/10.1021/acsami.2c11875

Read Online

ACCESS | Metrics & More | Article Recommendations | Supporting Information

ABSTRACT: With the advancement of material science and electronic technology, wearable devices have been integrated into daily lives, no longer just a stirring idea in science fiction. In the future, robust multifunctionalized wearable devices with low cost and long-term service life are urgently required. However, preparing multifunctional wearable devices robust enough to resist harsh conditions using a commercially available raw material through a simple process still remains challenging. In this work, reprocessable polyurea (HUBTPU) with a hard segment of hindered urea bonds (HUBs) and a soft segment of polyether is synthesized via a facile one-pot method. The robust dual functional wearable devices were obtained by simply spray-coating silver nanowires (AgNWs) on HUBTPU elastomer substrates. Due to the dynamic combination and decomposition of the HUBs and hydrogen bonds at 130 °C, the robust elastomer demonstrates favorable adhesion to various substrates. Especially, the partially embedded AgNW structure is also achieved by using ethanol as a spray solvent. The adhesion of HUBTPU substrates and embedded structure leads to stronger interfacial adhesion and stability compared to non-adhesive substrates. The as-obtained HUBTPU electrodes are able to be heated to 115 °C by applying a low voltage and sensing the strain deformation caused by human movement, which means that the electrodes are endowed with both electrical heating capability and strain sensing functionality. Therefore, this strategy reveals a potential way to prepare multifunctional wearable devices using other conductive particles and adhesive functional polymer substrates.

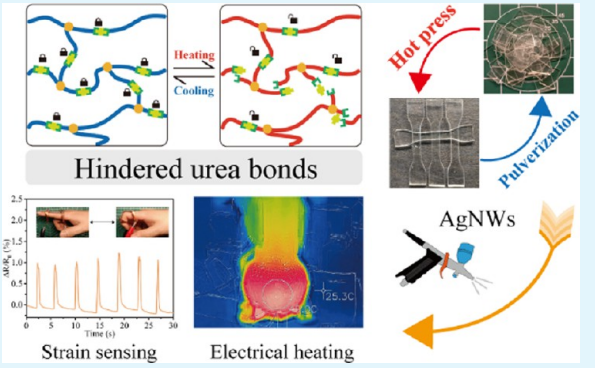

KEYWORDS: *hindered urea bonds, reprocessable polyurea, electrical heating, strain sensing, wearable device*

1. INTRODUCTION

In recent years, wearable devices gradually reveal amazing potential in different fields such as health monitoring, motion sensing, or injury prevention.[1,2] To construct wearable devices, stretchable electrodes serving as conductive pathways become the key elements.[3,4] Various techniques have been demonstrated to prepare diverse stretchable electrodes, such as incorporating ionic liquids into a polymer matrix to endow elastomers with conductivity,[5−9] utilizing a conductive polymer as a conductive pathway,[10,11] and integrating a polymer with rigid inorganic nanomaterials like carbon nanomaterials, MXenes, and metal nanowires.[12−16] Among all these different techniques, the combination of AgNWs and polymer substrates attracts exceptional attention in which AgNWs possess extremely low resistance, providing as-prepared electrodes favorable conductivity. The wide variety of polymers offers possibilities for electrodes to be functionalized. However, there are several stumbling blocks that are preventing us from preparing high-performance AgNWs and polymer-based stretchable electrodes, in which the interfacial adhesion problem is the most fatal one. Many efforts have been devoted to solve this problem, such as obtaining embedded structures by using the appropriate solvent to swell the substrate when spray coating,[17,18] using an adhesive material as an adhesive layer,[19] and employing chemical methods or plasma treatment to modify the surface of materials to increase adhesion by adding polar groups.[20,21] However, the strategies mentioned above lead to the complex manufacture process or insufficient adhesion strength when facing harsh conditions. Thus, demonstrating a facile strategy to solve the adhesion problem between AgNWs and polymer substrates remains challenging.

The property of substrates will have a direct impact on the performance of flexible electrodes. Consequently, the design of substrates holds great importance. A kind of favorable substrate is considered to possess suitable mechanical properties, facile synthesis process, and environmental friendliness, as well as being able to deal with the adhesion problem. The cross-linked

Received: July 4, 2022
Accepted: August 22, 2022

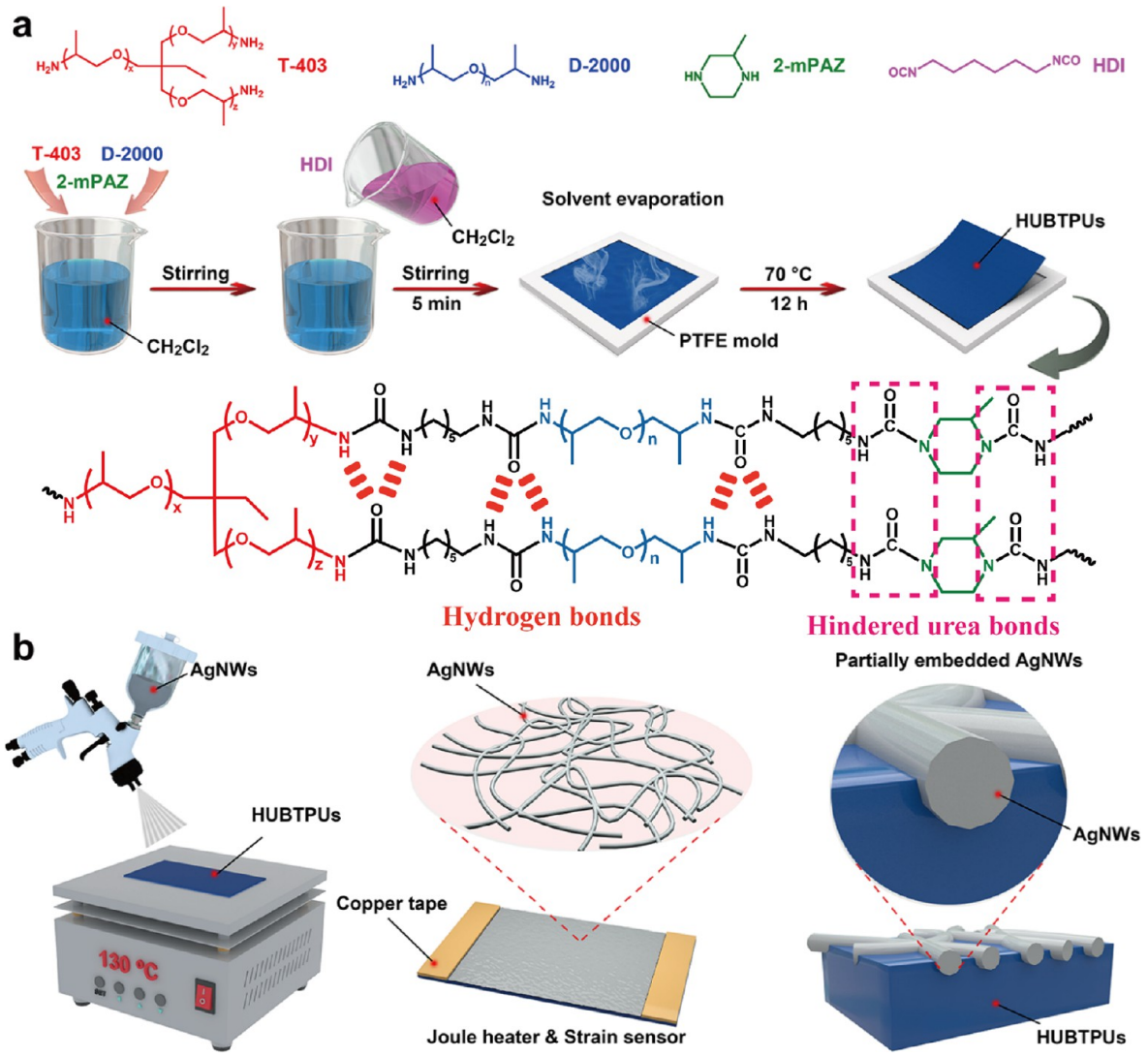

Figure 1. (a) Schematic demonstration of the synthesis of HUBTPUs. (b) Preparation of the dual functional wearable devices by spray-coating AgNWs on the HUBTPU substrates.

polymers feature better mechanical properties, heat resistance, and solvent resistance compared with thermoplastics due to the stable covalent bond networks. Meanwhile, the permanent cross-linked networks make it difficult to process and recycle, which result in great waste of energy resources and pollution of the environment.[22−24] Thus, finding a way to endow thermosets with reprocessability is rational. According to the literature, many attempts have been made to achieve this goal, including incorporate dynamic covalent bonds into the molecular structures. Up to now, a great variety of dynamic covalent bonds has been utilized to form dynamic covalent networks, such as retro-Diels−Alder,[25] reversible click chemistry,[26] reversible radical association−dissociation,[27] boronic ester exchange,[28] transcarbamoylation,[29] imine chemistry,[30,31] hindered urea bonds,[30,32−39] and disulfide metathesis.[40−42] However, the majority of them are limited for practical application by the usage of catalyst, expensive raw monomers, or complex synthesis methods. Hindered urea bonds (HUBs) are formed by introducing bulky substituents on one of the nitrogen atoms of a urea bond.[34] The HUBs are capable of being stable at room temperature and will dissociate at a higher temperature. This property is deemed to not only endow the substrate with dynamic nature but also exhibit good adhesive properties due to the secondary amino groups and isocyanate groups dissociated from HUBs, which are typical strong polar groups.[20] Recently, using HUBs to prepare reprocessable cross-linked polyurethane and polyurea is widely researched. For example, Cheng's group utilized 2-(*tert*-butyl amino) ethanol (TBAE) as a HUB monomer and dibutyltin dilaurate (DBTDL) as a catalyst to form a kind of poly(urea-urethane) (PUU) thermoset, which had comparable mechanical properties and remarkable recyclability. As-synthesized PUU maintained its original mechanical properties even after five times reprocessing.[34] Lei's group used lauric acid (LA) and trimethylolpropane tris[3-(2-methylaziridin-1-yl) propionate] (HD-100) to synthesize a cross-linker that had three imine groups. They further prepared a thermosetting polyurea vitrimer with reprocessability, permanent shape reconfiguration, and self-healing performance.[38] In short, the multifunctional polymer substrates have been widely achieved, manifesting the favorable tunability of HUB-based substrates. However, without conductivity, the application as wearable devices is impossible. Thus, the conductive electrodes composed of AgNW- and HUB-based substrates have been

https://doi.org/10.1021/acsami.2c11875
ACS Appl. Mater. Interfaces XXXX, XXX, XXX−XXX

demonstrated. Kang's group presented a transparent, flexible, and self-healable thermoacoustic loudspeaker prepared by spin-coating AgNWs on poly(urethane-hindered urea) (PUTPU)-containing HUBs.[17] Liu's group demonstrated cross-linked polyurea using polydimethylsiloxane as the soft segment and dynamic urea bonds serving as a self-healing elastomer substrate for coating and printing of AgNWs.[43] However, the progress mentioned before faces problems like the complex preparation process or single application. Thus, preparation of AgNW- and HUB-based durable multifunctional wearable devices through a facile way is still a challenge.

In this work, we demonstrated hindered urea bond-integrated polyurea (HUBTPU) substrates to prepare a kind of robust dual functional wearable device by spray-coating AgNWs at 130 °C, as shown in Figure 1a,b. The HUBTPU substrates were synthesized using commercially available raw materials of bifunctional polyether amine (D-2000) as the soft segment, hexamethylene diisocyanate (HDI) and 2-methylpiperazine (2-mPAZ) as the hard segment, and trifunctional polyether amine (T-403) as the cross-linking reagent, using dichloromethane as the solvent (Figure 1a, 2 2, and Table S1, Supporting Information). The obtained HUBTPU showed a high breaking strength of 18.8 MPa, an elasticity of 867%, and favorable reprocessability recovery (80% mechanical properties after three times reprocessing at 130 °C and 10 MPa for 60 min). The substrates also demonstrate strong adhesion to metals, which endows the as-prepared HUBTPU electrodes with better durability compared to embedded non-adhesive PDMS electrodes. The dual functions were realized, including electrical heating and strain sensing. The devices can reach a maximum temperature of 115.6 °C at a voltage of 2.5 V and maintain around 45 °C at 1.0 V, being able to maintain body temperature in the cold. With the strain sensing capability, the devices are capable of detecting the movement signal of a finger and elbow while remaining stable after the 800 times cycle test.

2. EXPERIMENTAL SECTION

2.1. Materials. 2-Methylpiperazine (2-mPAZ), polyvinylpyrrolidone (PVP; M_n = 40,000), and hexamethylene diisocyanate (HDI) were purchased from Adamas. Dichloromethane, ethanol, glycerol, and sodium chloride were supplied by Greagent. Deionized water was prepared in the laboratory. Trimethylolpropane tris[poly(propylene glycol), amine-terminated] ether (T-403, M_n = 440) was obtained from Macklin. Poly(propylene glycol) bis(2-aminopropyl ether) (D-2000, M_n = 2000) was bought from Aladdin. Silver nitrate was obtained from Chengdu Kelong Chemical Reagent Co., Ltd. (Chengdu, China). The polydimethylsiloxane (PDMS) prepolymer (Sylgard 184A) and the curing agent (Sylgard 184B) were purchased from Dow Corning Corporation. All reagents were used without further purification.

2.2. Synthesis of HUBTPUs. Taking HUBTPU-2 as an example, 0.250 g of 2-mPAZ, 2.200 g of T-403, and 5.000 g of D-2000 were dissolved in 20 mL of dichloromethane by magnetic stirring in a 100 mL beaker. Then, 2.100 g of HDI was also dissolved in 20 mL of dichloromethane and added into the beaker mentioned before to obtain a homogeneous clear solution. After 5 min of stirring, the solution was transferred into a square Teflon mold, and dichloromethane was evaporated slowly at room temperature for 12 h. After most of the solvent had evaporated, the mold was transferred to a vacuum oven and baked at 70 °C for 12 h. Finally, HUBTPUs were obtained and stored in a dry dish for later use.

2.3. Reprocess Experiment. The samples of HUBTPU-2 were cut into many pieces by a blade, and then the pieces were hot-pressed at 130 °C and 10 MPa for 60 min. The as-prepared samples were cooled to room temperature and named 1 recycled reprocessing sample. Repeating the above process, the 2 recycled reprocessing samples and 3 recycled reprocessing samples were obtained.

2.4. Synthesis of AgNWs. AgNWs were prepared according to the reported method.[44] First, 5.86 g of PVP was dissolved in 200 mL of glycerol using a 500 mL round-bottom flask with mechanical stirring at 100 °C; after 4 h, a transparent and homogeneous solution was formed. When the solution was cooled to room temperature, $AgNO_3$ (1.58 g) was added, and after 6 h of stirring, the solution turned to yellow. Then, 10 mL of glycerol solution containing 59 mg of NaCl and 0.5 mL of H_2O was added into the flask. After all these steps, the flask was put into an oil bath, which was heated to 210 °C. The solution turned to gray-green in 40 min. Finally, when the flask was cooled to room temperature, 200 mL of H_2O was added. Then, the mixture was centrifuged at 4000 rpm for 20 min. The precipitation was washed by water for three times to remove PVP residues. The prepared AgNWs were dispersed in an appropriate amount of ethanol to form AgNW solution with a concentration of 1 mg/mL. A SEM image of the obtained AgNWs is shown in Figure S1; the average length was about 20 μm and the average diameter was about 100 nm, which was the same as reported.

2.5. Preparation of HUBTPU Electrodes. As a substrate, HUBTPU-2 was cut into a 2 × 5 cm rectangle and put on a hot plate, which was set at 130 °C. Ten milliliters of 1 mg/mL AgNW ethanol dispersions was spray-coated on each HUBTPU-2 substrate using a spray gun, and the distance from the muzzle to the substrate was about 10 cm. To connect power and test equipment conveniently, two copper foils were fixed on both sides of the substrate. The as-prepared devices were used for electrical heating and strain sensing.

2.6. Preparation of the Embedded and Spray-Coated PDMS Electrodes. AgNWs were spray-coated on a PTFE mold first, the uncured PDMS (the mass ratio of Sylgard 184A and Sylgard 184B was 10:1) was poured into the mold, and then the mold was incubated at 70 °C for 3 h. After PDMS was cured, the mold was peeled off and embedded PDMS electrodes were prepared. Also, the spray-coated PDMS electrodes were prepared by spray-coating AgNWs onto the cured PDMS films at 100 °C. The amount of AgNWs was the same as when preparing HUBTPU electrodes.

2.7. Characterization and Measurements. Fourier transform infrared spectroscopy (FTIR) was conducted by a Nicolet iS50 FTIR spectrometer in a wide range of 400−4000 cm^{-1}. The temperature-dependent in situ infrared absorption spectra of HUBTPU-2 were conducted by heating from 30 to 200 °C at 5 °C/min under nitrogen protection. Dumbbell specimens (gauge length × width × thickness: 15 × 4 × 1.0 mm^3) were made to test the mechanical behavior of HUBTPUs and reprocessed samples using a tensile apparatus (Instron 5567) with a sensor of 1KN, and the stretch rate was set to 100 mm/min for all samples. Differential scanning calorimetry (DSC) was utilized to determine the glass transition temperature of HUBTPUs with a NETZSCH DSC 204 F1 instrument. Dynamic mechanical analysis (DMA) was proceeded with a DMA Q800 instrument (USA) under tensile mode with a constant strain of 5%, the tan δ curve was obtained at a frequency of 1 Hz and a strain of 0.1%, and heating ramps were 3 °C/min from −100 to 180 °C. To analyze the thermal performance of HUBTPUs, thermogravimetric analysis (TGA) was conducted using an SDT-Q600 (TA, American) from 25 to 600 °C at a heating rate of 10 °C/min under a N_2 atmosphere. The surface and cross-sectional morphology was observed using SEM (JSM-5900LV, JEOL, Japan) at an accelerating voltage of 5 kV. EDS (EDAX Octane Elect Super) was also used to further study the element composition of the cross section. Electric heating performance was tested by an infrared thermal imager (FLIR ONE). The strain sensing performance was recorded by a Keithley 2450 source meter under a constant voltage of 0.1 V.

3. RESULTS AND DISCUSSION

3.1. Preparation and Characterization of HUBTPUs. Due to the various advantages of thermosets and HUBs mentioned before, it is rational for us to design a thermoset

https://doi.org/10.1021/acsami.2c11875
ACS Appl. Mater. Interfaces XXXX, XXX, XXX−XXX

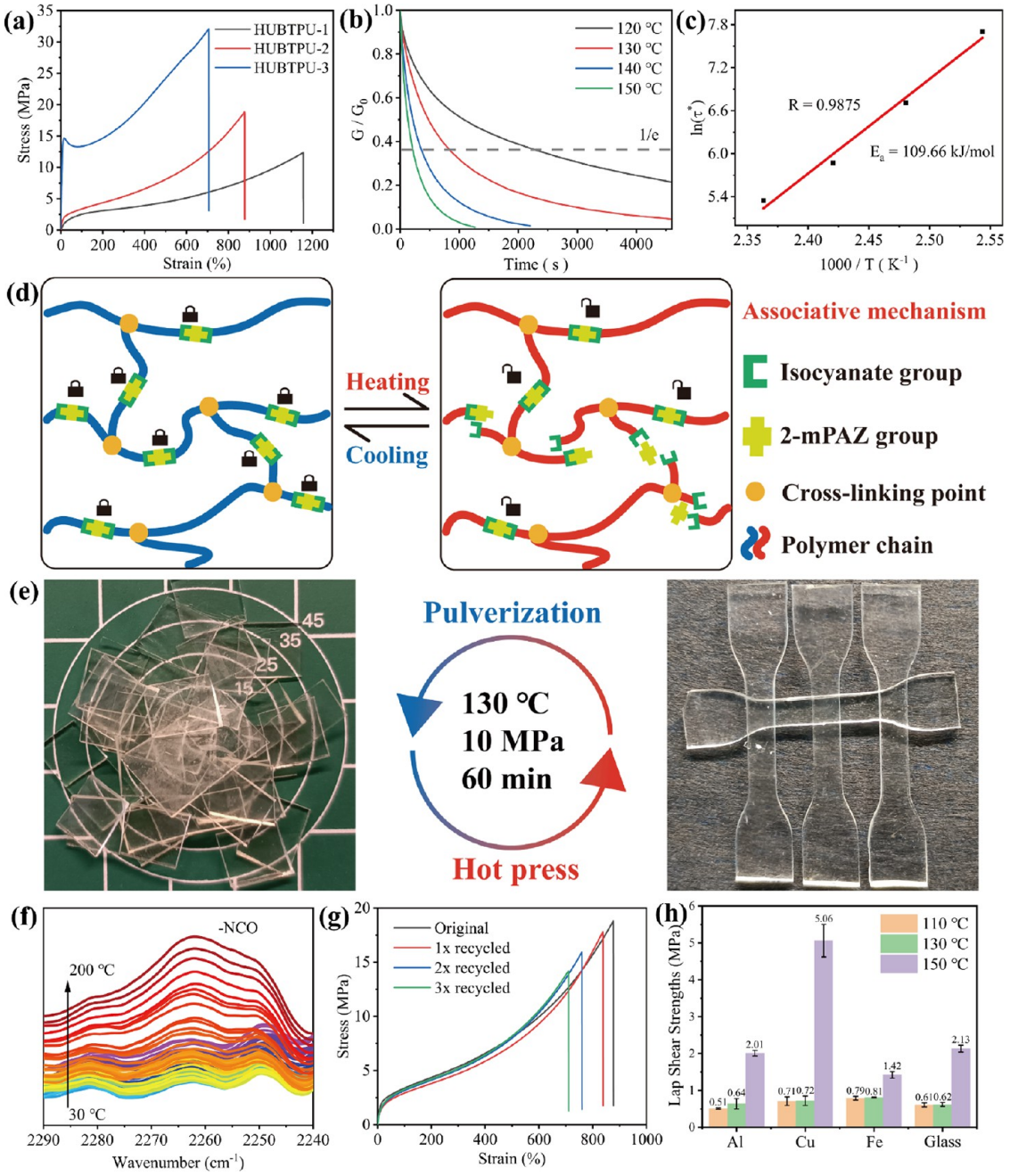

Figure 2. (a) Stress−strain curves of HUBTPU-1, HUBTPU-2, and HUBTPU-3. (b) Stress relaxation analysis of HUBTPU-2 at various temperatures. (c) Fitting of relaxation time−temperature to an Arrhenius equation. (d) Reversible exchange mechanism of hindered urea bonds. (e) Photographs of the recyclability of HUBTPU-2 via hot press after multiple times under 10 MPa at 130 °C for 60 min. (f) FTIR spectra of HUBTPU-2 between 30 and 200 °C. (g) Stress−strain curves of the original and multiple recycled HUBTPU-2 samples. (h) Lap shear strengths between HUBTPU-2 and various substrates bonded at 110, 130, and 150 °C.

elastomer based on HUBs as the substrates of wearable devices. Consequently, commercially available materials, including D-2000, T-403, 2-mPAZ, and HDI, were selected to synthesize various cross-linked HUBTPUs. They were prepared according to the recipes listed in Table S1. Utilizing the fast reaction feature between isocyanate and amine, we are able to obtain HUBTPUs through one-pot synthesis, which is considered as a great advantage for HUBTPUs to face industrial production. To prove the cross-linked structure of HUBTPUs, swelling test was conducted. HUBTPU-2 was put into different solvents at room temperature. After 48 h, the elastomers remained insoluble, as shown in Figure S2, indicating the cross-linked structure of HUBTPUs. To further investigate the structure of HUBTPUs, the gel content was tested by using a Soxhlet extractor and dichloromethane as a solvent for 48 h. As demonstrated in Figure S3, the gel content gradually rose with the increase in 2-mPAZ content, from 76.83% for HUBTPU-1 to 92.59% for HUBTPU-3, which suggested that the higher 2-mPAZ content led to a higher cross-linking degree of HUBTPUs. The chemical structure of monomers and HUBTPUs was confirmed by the FTIR spectra. As presented in Figure S4, for T-403, D-2000, and 2-mPAZ, the characteristic peaks at 3000 and 1600 cm^{-1} are attributed to the stretching and bending vibrations of $-NH_2$

https://doi.org/10.1021/acsami.2c11875
ACS Appl. Mater. Interfaces XXXX, XXX, XXX−XXX

and −NH−, respectively. The stretching vibration peak at about 1100 cm^{-1} was found in T-403 and D-2000 corresponding to the C−O−C structure. Notably, the characteristic peak of HDI at 2275 cm^{-1} was ascribed to isocyanate groups and then disappeared in HUBTPU-2; combining the fact that the characteristic peaks at 3361, 1633, and 1564 cm^{-1} corresponding to the stretching and bending vibrations of urea bonds showed up in HUBTPU-2, the successful synthesis of HUBPUS-2 was confirmed.[32] Also, there is no significant difference between HUBTPUs in the FTIR spectra, as shown in Figure S5. Considering the practical usage of HUBTPUs as wearable electrical devices, mechanical performance needs to be tested first. As demonstrated in Figure 2a, by increasing the molar fraction of 2-mPAZ and D-2000 from 1:3 for HUBTPU-1 to 1:1 for HUBTPU-2 and 3:1 for HUBTPU-3 (Table S1), the breaking strength increased dramatically from 12 to 32 MPa; meanwhile, the breaking elongation decreased gradually from 1155 to 705%. These changes could be attributed to the fact that the rigidity of the six-membered ring structure belongs to 2-mPAZ, which was much greater than that of the ether bond belonging to D-2000. Generally speaking, the existence of a rigid structure will improve the plasticity of polymers. Macroscopically, HUBTPU-1 is too easy to be bent or stretched and HUBTPU-3 is so hard that it could not be bent by human joint movement. Consequently, HUBTPU-2, which is not too hard and is not easily deformed, is selected to be applied to the following tests and preparation of electrical devices.

In practice, continuous bending of the substrate was unavoidable. Thus, cyclic tensile test was conducted with five successive load−unload cycles at 50% strain to characterize the hysteresis and elasticity of HUBTPU-2, as demonstrated in Figure S6a. The first cycle had the largest hysteresis loop, indicating successful energy dissipation of HUBTPU-2, and the hysteresis loop slightly decreased in the last three cycles compared to the second cycle. This result could be attributed to the fact that there was not enough time for the recovery of dissociation, microstructures, and the orientation of segment domains or the reformation of hydrogen bonds because of hysteresis effects.[45,46] As shown in Figure S6b, cyclic tensile test was conducted with seven successive load−unload cycles as the strain gradually increased from 50 to 600%, which was intended to further investigate the toughness and elasticity of HUBTPU-2. The results demonstrated that residual strain existed in every cycle, which could be explained by the fact that during the stretching process, the broken hydrogen bonds formed new bonding points. However, the cross-linked structure of HUBTPU-2 restricted the further movement of molecular chains; thus, the residual strain gradually decreased with increasing strain.[47,48] All in all, the results of the cyclic stretching experiment proved that HUBTPU-2 had good toughness and elasticity, which could be attributed to its cross-linked structure and hydrogen bonds and available as a substrate of wearable electrical devices. Serving as a substrate of wearable electrical devices, which had a heating function, the thermal stability of HUBTPU-2 was characterized. As shown in Figure S7, TGA results showed that the initial decomposition temperature of HUBTPU-2 reached as high as 316.9 °C, much higher than the operating temperature of general wearable devices. The storage modulus and loss modulus were measured by DMA to demonstrate the elasticity of HUBTPU-2, as shown in Figure S8. Similar to other elastomers, a rubbery plateau was found at about room temperature, proving the good elasticity. The elastomer samples retained solidlike behavior as the storage modulus always remained higher than the loss modulus.[49] As a traditional polymer material, the characterization of glass transition temperature (T_g) is indispensable. As demonstrated in Figure S9, the T_g of HUBTPUs was measured simultaneously by DSC and DMA. The first T_g at about −58 °C of HUBTPUs is attributed to the soft segment constructed by D-2000 polyether. The second T_g values at 11.4, 29.2, and 57.0 °C for HUBTPU-1, HUBTPU-2, and HUBTPU-3, respectively, belong to the hard segment. The rise in hard segment T_g can be explained as the rigidity improvement of the hard segment molecular chain with the increase in 2-mPAZ content. As to the endothermic peak from 30 to 100 °C in DSC curves of HUBTPUs, it is ascribed to the activation of the HUBs.[32]

It is generally acknowledged that the hindered urea bonds follow the associative mechanism, which means that as the temperature increases, urea bonds tend to dissociate into secondary amine groups and isocyanate groups, and at the same time, secondary amine groups and isocyanate groups will also reform urea bonds.[35,50,51] When the temperature reaches the active range of HUBs, the macroscopic properties of the material change. Such a storage modulus of HUBTPU-2 decreases sharply from 20 to 70 °C (Figure S8), corresponding to an endothermic peak found at about 60 °C in the results of the DSC test (Figure S9). Thus, the active temperature of as-prepared HUBTPUs is considered at 60 °C, which is similar to other reported HUBs.[30,32,52−54] The temperature dependence of the thermal expansion curve of HUBTPU-2 demonstrated in Figure S10 further confirms the T_g and the active temperature of HUBs. The curve clearly shows that the T_g is −52.8 °C and the topology freezing-transition temperature (T_v) is 81.2 °C. The result of T_g demonstrates no significant difference from the previous test results, and the T_v is higher than the active temperature of HUBs. This could be attributed to the fact that the active temperature of HUBs is not an exact temperature point but a wide temperature range, which could be proved by the wide endothermic peak measured by DSC starting from about 20 to 130 °C (Figure S9).

3.2. Recyclability and Adhesive Properties. HUBs could not only regulate the mechanical properties of HUBTPUs but also endow HUBTPUs with dynamic properties, as illustrated in Figure 2d. The HUBs participate in formation of a cross-linked network at the operating temperature and decompose to 2-mPAZ groups and isocyanate groups at higher temperature, and then the cross-linked structure is broken and becomes linear-like thermoplastics. Such a dynamic property endowed HUBTPUs with reprocessability, which makes the HUBTPUs environmentally friendly. To further investigate dynamic properties of the HUBs, the time- and temperature-dependent stress relaxation behavior of HUBTPU-2 was conducted by DMA. As shown in Figure 2b, the relaxation modulus was monitored as a function of time from 120 to 150 °C. Also, the stress relaxation of HUBTPU-2 accelerated as the temperature increased, which could be attributed to the rapid dissociation of dynamic HUBs. By convention, the relaxation time (τ^*) was defined as 1/e of the moralized relaxation modulus. According to τ^* and the corresponding temperature, the activation energy (E_a) of the dynamic HUBs was calculated as 109.66 kJ/mol (Figure 2c) by the Arrhenius equation, which is higher than that of more sterically hindered 2,6-dimethylpiperazine and lower than that of less sterically hindered piperazine (Table S2). The topology

https://doi.org/10.1021/acsami.2c11875
ACS Appl. Mater. Interfaces XXXX, XXX, XXX−XXX

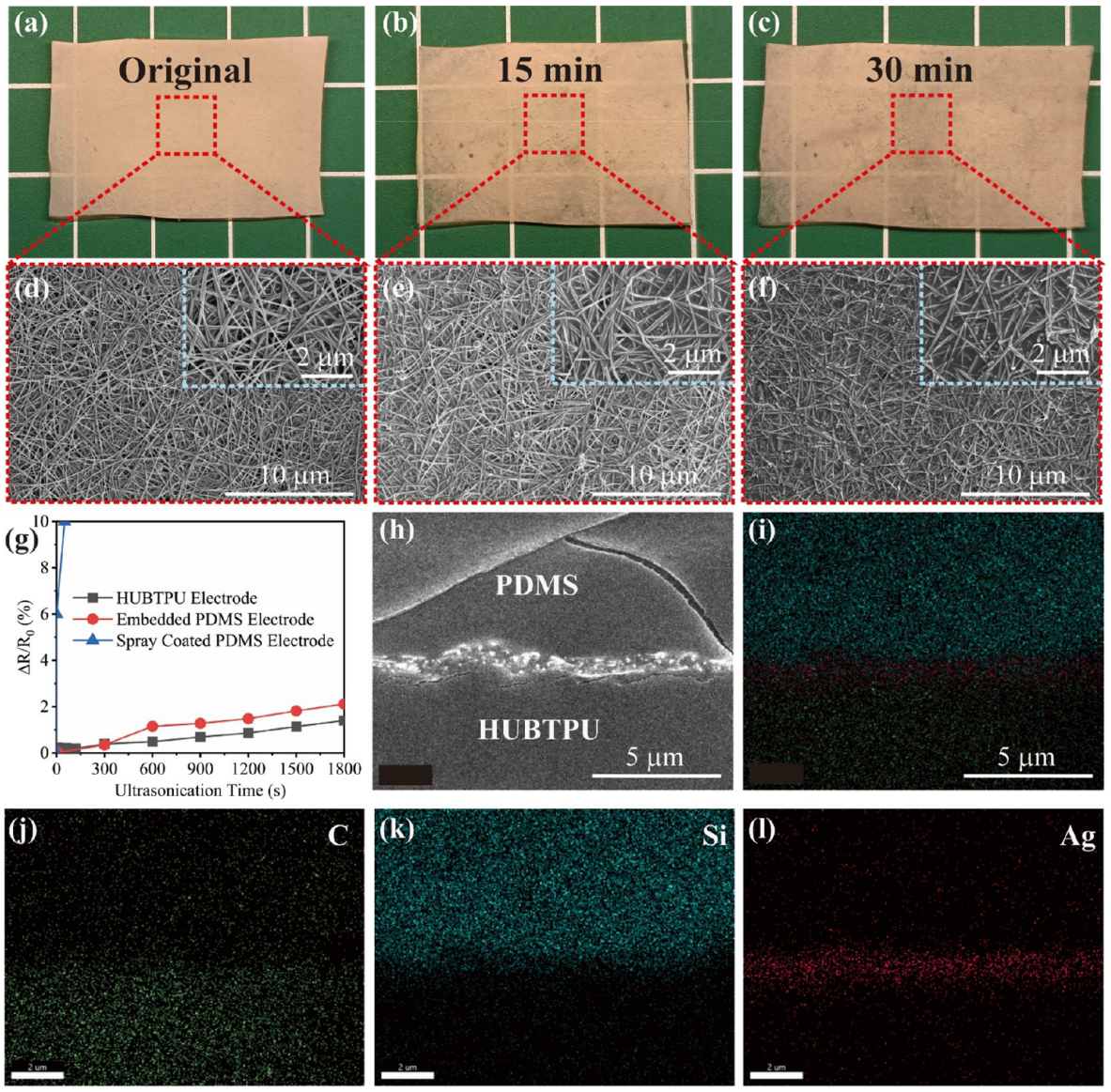

Figure 3. (a–c) Photographs of the original stretchable electrodes (a) after 15 min of sonication (b) and after 30 min of sonication (c). (d–f) SEM images of the original stretchable electrodes (d) after 15 min of sonication (e) and after 30 min of sonication (f). The inset images are enlarged views of the corresponding images. (g) Sheet resistance of the HUBTPU electrode, embedded PDMS electrode, and spray-coated PDMS electrode during sonication. (h) SEM image of the cross section of the PDMS-packaged HUBTPU electrode. (i–l) Corresponding EDS images of the cross section of the PDMS-packaged HUBTPU electrode.

freezing-transition temperature (T_v) of HUBTPU-2 was also measured by DMA as 81.2 °C, and the T_g was further confirmed as −52.8 °C as shown in Figure S10. Below the T_v, the network topography configuration will be quenched and, above the T_v, it will be triggered; when T_v is higher than T_g, the material may be able to be reprocessed above T_v.[32] To further prove the dynamic nature of HUBs, the FTIR spectra of HUBTPU-2 between 30 and 200 °C are demonstrated in Figure 2f. The peak at 2265 cm^{-1} corresponding to the isocyanate groups gradually became higher as the temperature rose, indicating the dissociation of HUBs and formation of isocyanate groups.

The dynamic nature of HUBs endows cross-linked HUPTPUs with reprocessability. As demonstrated in Figure 2e, HUBTPU-2 was pulverized into pieces and then reprocessed into homogeneous dumbbell-shaped specimens through hot pressing at 130 °C under 10 MPa for 60 min. This process successfully underwent for three times, which strongly proved the dynamic nature of the HUBs. Reprocessed samples were further investigated, as shown in Figure 2g; the stress–stain curves of original and reprocessed HUBTPU-2 exhibit good mechanical property recovery. The recovery rates of tensile strength and elongation at break were quantified. The results show that the tensile strength and elongation at break both decreased slowly during three times reprocessing but maintained about 80% compared to the original. To investigate the reason why HUBTPU-2 maintained excellent mechanical properties, multiple tests were conducted. First, FTIR was conducted to investigate the chemical structure of HUBTPU-2 after reprocessing. As demonstrated in Figure S11, nearly nothing changed in these curves, manifesting the chemical structure of HUBTPU-2 after reprocessing remained stable. The gel content was tested with the usage of a Soxhlet extractor and dichloromethane, and the result is shown in

https://doi.org/10.1021/acsami.2c11875
ACS Appl. Mater. Interfaces XXXX, XXX, XXX–XXX

Figure S12. After three times reprocessing, the gel content of HUBTPU-2 gradually increased from 87 to 93%, manifesting that the structure of HUBTPU-2 stayed cross-linked. The storage modulus of three times recycled HUBTPU-2 was tested by DMA, and the result showed a slight decrease compared to the original as shown in Figure S13. Interestingly, the storage modulus decreases with increasing gel content after multiple times reprocessing. To explain this phenomenon, a schematic demonstration of a hypothetical degradation mechanism of the HUBTPU is shown in Figure S14. As the HUBTPU is synthesized, unreacted isocyanate end groups readily react with ambient water to form amino groups and carbon dioxide, leaving amino-terminated linear structures and cross-linked structures mixed together.[51] During the hot press, a part of active isocyanate groups could react with the terminal amino-forming stable urea bonds. After cooling, a part of linear chains connects to the cross-linked network and the degree of cross-linking reduced, which results in an increase in gel content and a decrease in storage modulus simultaneously. At last, to investigate the T_g of three times recycled HUBTPU-2, the DSC and DMA tests were carried out, and the results are shown in Figure S15. The T_g of the soft segment remained as low as −58.6 and −54.8 °C measured by DSC and DMA, respectively, and the T_g of the hard segment dropped slightly from 29.2 to 27.1 °C, which could be attributed to the degeneration of the structure of the hard segment. All the evidence manifested that the dynamic nature endowed HUBTPU-2 with good reprocessability.

Based on the dynamic behavior and good mechanical properties of HUBTPU-2, excellent adhesive properties were expected, which was helpful in enhancing the interface adhesion problem between AgNWs. To explore the adhesion property of HUBTPU-2, the common materials of Al, Cu, Fe, and glass sheets were used and bonded under different temperatures, and the result is demonstrated in Figure 2h. The lap shear strength between HUBTPU-2 and driverse objects under different bonding temperatures was all greater than 0.51 MPa (tested with Al sheets bonded at 110 °C) and reached a maximum value of 5.06 MPa when HUBTPU-2 was tested with Cu sheets bonded at 150 °C. It is very obvious that the adhesion of HUBTPUs to all substrates is greatly improved when the bonding temperature reaches 150 °C, which is attributed to the fact that the HUBTPU is easier to fit perfectly with the microstructure of the substrate surface at higher temperatures. All results were manifesting that HUBTPU-2 showed a good adhesive property, indicating the potential to form great interfacial adhesion with AgNWs.

3.3. HUBTPU-Based Dual Functional Wearable Devices. Polar groups such as secondary amino groups and isocyanate groups are beneficial for improving the adhesion between substrates and AgNWs.[20] Thus, it was rational to choose 130 °C as the spray coating temperature since secondary amino groups and isocyanate groups would show up due to the dynamic nature of HUBs. To obtain an embedded structure, ethanol was chosen to disperse AgNWs, which swelled HUBTPU-2 better than other solvents (Figure S2).[17,43] After completing the spray coating step in accordance with the above conditions, the dual functional wearable devices based on HUBTPU-2 were prepared. To clearly illustrate the contribution of the adhesion to electrode stability, non-adhesive PDMS was selected as the counterpart. Two kinds of typical electrode preparation methods are demonstrated: spray coating AgNWs on cured PDMS and spray coating AgNWs on the PTFE mold first and then curing PDMS on the mold. Through these two methods, the spray-coated PDMS electrode and the embedded PDMS electrode were prepared. To investigate the adhesion between electrodes and AgNWs, the as-prepared electrodes were sonicated in an aqueous solution at room temperature. The SEM images of counterpart electrodes before and after sonication are demonstrated in Figure S16. It is evident that the AgNWs on the spray-coated PDMS electrode are removed completely. On the contrary, the AgNWs embedded in PDMS remained stable after sonication, manifesting that the embedded structure is important to enhance the stability of the electrodes. As demonstrated in Figure 3a−c, the as-prepared HUBTPU electrodes were covered uniformly by abundant AgNWs. Also, after sonication for 15 and 30 min, a small portion of AgNWs was removed from the surface, but most of AgNWs were left on the surface. The result was further confirmed by SEM images as shown in Figure 3d−f, and the AgNWs of as-prepared HUBTPU electrodes were the same as the AgNWs that were just synthesized (Figure S1). After 15 min of sonication, AgNWs started to degrade, becoming shorter and forming silver nanoparticles. This trend became more pronounced after 30 min of ultrasound treatment; less long AgNWs remained on the surface and short AgNWs and silver nanoparticles thrived. Interestingly, the $\Delta R/R_0$ of HUBTPU electrodes remained more stable compared to other electrodes (Figure 3g), the spray-coated PDMS electrode was destroyed instantly due to the low adhesion between PDMS and AgNWs, and the embedded PDMS electrode remained much more stable due to the embedded structure. This result manifests that the HUBTPU electrodes are more stable than the other two electrodes, which can be attributed to two points: First, the abundant AgNWs tightly bonded to HUBTPU enabled the conductive pathway to remain, even though the AgNW structure was partially damaged. Second, the conductive pathway formed by embedded AgNWs was more resistant to ultrasound damage. To prove that the embedded structure was formed, the cross-sectional SEM images of the HUBTPU electrode are demonstrated in Figure S17a,b. The AgNWs and HUBTPU are messed up, and it is hard to find a clear boundary between them. We attributed this to the brittle fracturing process conducted by liquid nitrogen and took the SEM images of the surface of the liquid nitrogen brittle fractured samples as shown in Figure S17c,d. It is clear that the surface of brittle fractured samples is destroyed compared to the surface of as-prepared samples (Figure 3d). The destruction of the surface could be ascribed to the mismatched thermal expansion coefficients of AgNWs and HUBTPUs; as the temperature decreases, the volume of HUBTPU as a polymer shrinks greatly, while the volume of AgNWs remains unchanged, which causes the stress generated at the interface to damage the surface of the electrode. Thus, to have a clear view of the cross section, PDMS was cured on the surface of the HUBTPU electrode to protect the surface structure from being destroyed by liquid nitrogen. To distinguish PDMS from HUBTPU, EDS images are shown in Figure 3i−l. In the place where Ag (rad, corresponding to AgNWs) is the most concentrated, Si (blue, representing PDMS) and C (green, representing HUBTPU) are distributed evenly at the same time, manifesting that the AgNWs are existing on the surface and are embedded under the surface of the HUBTPU substrate simultaneously. All the above results manifested that AgNWs firmly bonded with the HUBTPU substrate,

https://doi.org/10.1021/acsami.2c11875
ACS Appl. Mater. Interfaces XXXX, XXX, XXX−XXX

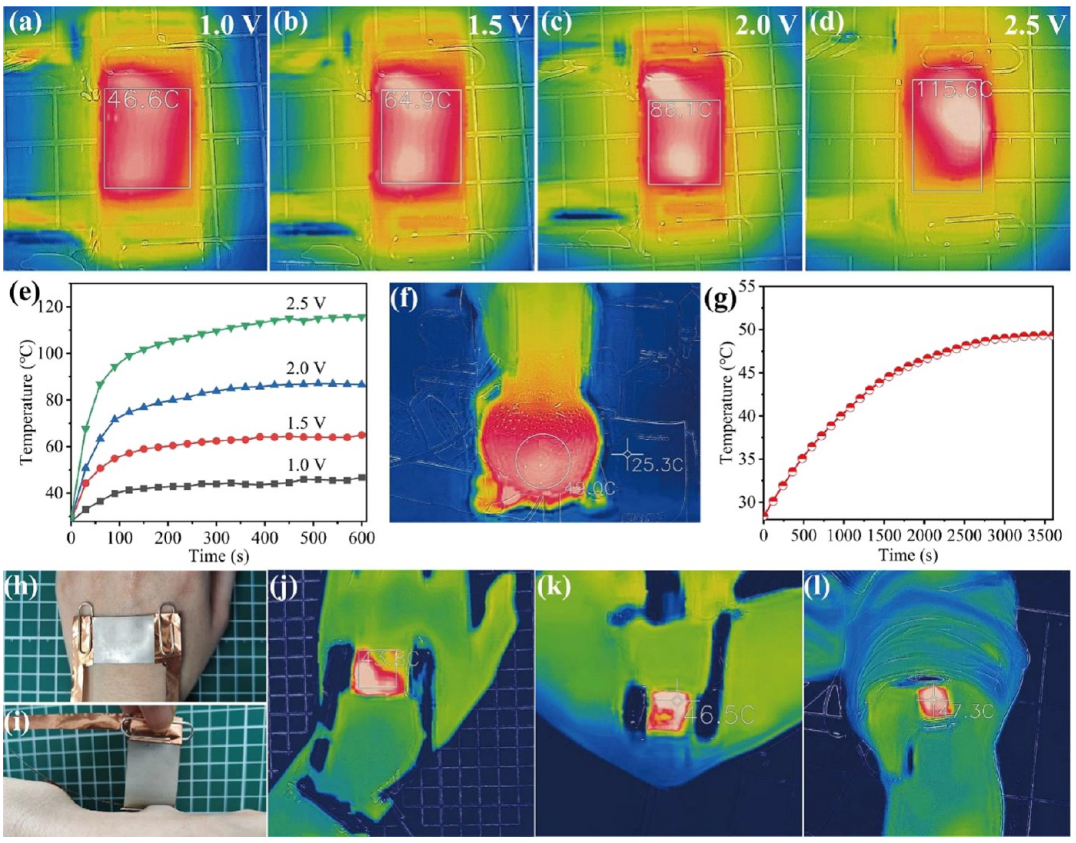

Figure 4. (a–d) Infrared thermal imaging photos of the working electrical heaters at 1.0 V (a), 1.5 V (b), 2.0 V (c), and 2.5 V (d). (e) Plot of the temperature versus time at various applied voltages of the as-prepared electrical heaters. (f) Infrared thermal imaging photo of heating of 25 mL of water. (g) Curve of the temperature increasing with time when heating 25 mL of water. (h) Photograph of the as-prepared electrical heating device sticking to the back of the hand. (i) Peeling from the back of the hand. (j–l) Infrared thermal imaging photos of heating of the hand (j), elbow (k), and knee (l).

which was ascribed to the interfacial adhesion and embedded structure.

Since the sheet resistance of as-prepared HUBTPU electrodes was as low as about 1 Ω/sq., which was attributed to the extradentary conductivity of AgNWs, the electrical heating capability of HUBTPU electrodes was expected. Consequently, to investigate the electrical heating performance, two copper foils are fixed on both sides of HUBTPU electrodes by clips for connection to external test equipment. Then, a DC power supply was used to apply different specific voltages to the HUBTPU electrodes, the temperature raised dramatically in first 100 s, and after that, the temperature of every different specific voltage remained stable as demonstrated in Figure 4e. Specifically, the temperature of HUBTPU electrodes raised to 46.6 °C, which was warm and comfortable for the human body when applying a voltage of 1.0 V, measured by an infrared thermal imager as demonstrated in Figure 4a. Moreover, when the voltages were up to 1.5 and 2.0 V, the temperatures gradually increased to 64.9 and 86.1 °C, respectively (Figure 4b,c). The highest temperature reached 115.6 °C at a voltage of 2.5 V as shown in Figure 4d. We did not increase the voltage further because when the HUBTPU electrodes were heated up, the HUBTPU substrates behaved differently compared to room temperature. Intuitively, the HUBTPU electrodes became more and more soft and sticky during the heating process, which could be ascribed to the fact that the modulus of HUBTPU-2 substrates decreased dramatically in the temperature range from 25 to 75 °C (Figure S8). The HUBs started to decompose into amino groups and isocyanate groups, which are often used as an adhesive. It is worth mentioning that the highest temperature achieved by electrical heating was still far from the maximum temperature that HUBTPU-2 substrates could withstand, which was higher than 200 °C (Figure S7). To further investigate the heating performance of HUBTPU electrodes, a HUBTPU electrode was attached to the bottom of a 25 mL round-bottom flask, which was filled with 20 mL of water, and then a voltage of 2.0 V was applied. As demonstrated in Figure 4f,g, the water was finally heated to 49.0 °C after about 60 min, manifesting the favorable electrical heating capability of HUBTPU electrodes. Furthermore, HUBTPU electrodes were attached to different parts of the skin surface to serve as wearable devices. As shown in Figure 4h, a HUBTPU electrode was affixed to the back of the hand, and it was able to adhere to the skin without additional fixation, which is attributed to the adhesiveness of the HUBTPU-2 substrate itself (Figure 4i). To quantitatively characterize the adhesion of HUBTPUs to organic surfaces, the peeling strength between the HUBTPU and the human skin was conducted. As demonstrated in Figure S18, the peeling strength reaches 40 N m^{-1}, which is enough for our device to attach to the human body. Taking advantage of this property, HUBTPU electrodes were adhered to the back of the hand, elbows, and knees and heated by a voltage of 1 V. The resulting inferred images are demonstrated in Figure 4j–l; the HUBTPU electrodes reached about 45 °C during the test, indicating that the HUBTPU

https://doi.org/10.1021/acsami.2c11875
ACS Appl. Mater. Interfaces XXXX, XXX, XXX–XXX

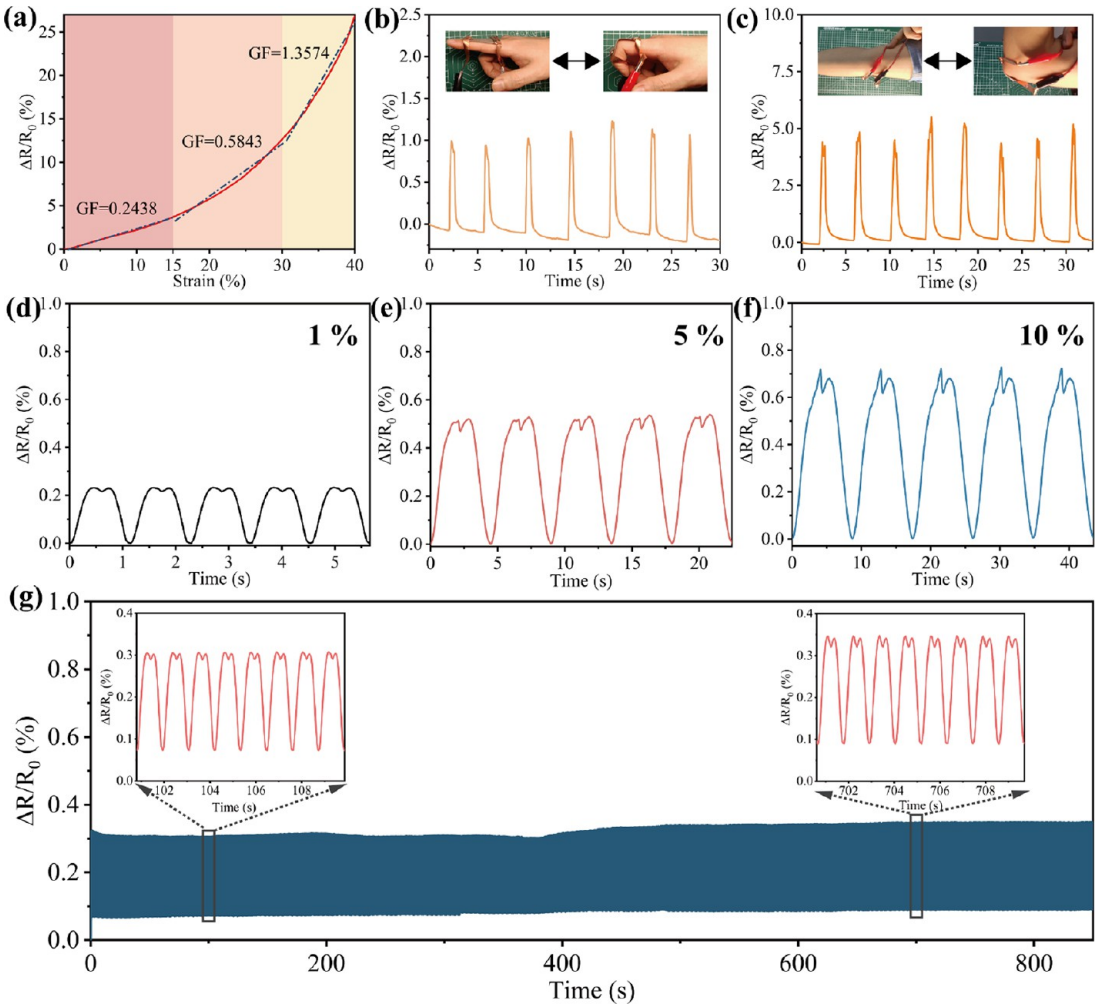

Figure 5. (a) Resistance variation of the as-prepared strain sensors on applied tensile strain. Gauge factors (GFs) were obtained by fitting the curve with three segments (0−15, 15−30, and 30−40% strain). (b, c) Images and $\Delta R/R_0$ variation when different reversible bending movements were applied by a finger (b) and elbow (c). (d−f) Images of $\Delta R/R_0$ variation when applying 1% strain (d), 5% strain (e), and 10% strain (f). (g) Periodical $\Delta R/R_0$ variation upon stretching−releasing cycles (1% strain).

electrodes had the potential to assist users in maintaining the temperature in cold conditions, which was a serviceable function of the wearable devices.

During the deformation of HUBTPU electrodes like bending and stretching, a relative displacement occurs between AgNWs, resulting in a variation in the overall resistance of HUBTPU electrodes, which would endow HUBTPU electrodes with the function of strain sensing. Also, strain sensing will make it possible to sense human body movements, which is concerned as a practical function for wearable devices. Thus, it is rational to investigate the performance of HUBTPU electrodes used as strain sensors. Figure 5a shows the relative change in resistance $(\Delta R/R_0)$ as a function of the strain (ε) of HUBTPU electrodes. The gauge factor (GF), which is defined as the slope of the $(\Delta R/R_0)$ versus ε plot, is an indispensable parameter for investigating the sensitivity of strain sensors. For the HUBTPU electrodes, the mathematical fit of the $(\Delta R/R_0)$ versus ε plot generates three different slopes of 0.24, 0.58 and 1.36 corresponding to the strain from 0 to 15%, 15 to 30%, and 30 to 40%, respectively. The upper limit of strain is set at 40% because excessive strain will destroy the network structure of AgNWs and 40% strain is sufficient for wearable applications. To verify the capability of HUBTPU electrodes to be used as a wearable soft sensor to monitor diverse human body motions, HUBTPU electrodes were adhered to fingers and elbows as shown in Figure 5b,c. When the fingers and elbows were kept straight, HUBTPU electrodes were neither stressed nor deformed, so the resistance was kept to a minimum level. As the fingers and elbows were bent, HUBTPU electrodes became deformed and the contact between AgNWs deteriorated, leading to the sudden increase in $(\Delta R/R_0)$. The greater change in $(\Delta R/R_0)$ due to the flexion of the elbow could be attributed to the greater strain created when the elbow was flexed. As a result, the movement of bending fingers and elbows is perfectly transformed into electrical signals, manifesting that the HUBTPU electrodes are able to sense human movements. To further investigate the sensing capability of HUBTPU electrodes, successive cyclic extension and release test was conducted by setting strain values of 1, 5, and 10% (Figure 5d−f), and not surprisingly, all different strains were well detected; also, with the increase in strain, the peak value of $(\Delta R/R_0)$ also increases gradually. The response time and recovery time of HUBTPU electrodes are demonstrated in Figure S19. The response time and recovery time were measured as 0.28 and 0.32 s, respectively, which were quick enough to detect human movement. As a wearable strain

https://doi.org/10.1021/acsami.2c11875
ACS Appl. Mater. Interfaces XXXX, XXX, XXX−XXX

sensor, the cycling stability is very important as this directly affects the service life of the device. Thus, successive cyclic extension and release test was conducted with a strain of 1% for about 800 times (Figure 5g). The result shows that even after 800 times deformation, the sensitivity of HUBTPU electrodes nearly remains unchanged, manifesting that HUBTPU electrodes possess favorable cycling stability. Compared with other sensors reported in the literature that use AgNWs as a conductive component, the as-prepared strain sensor possesses ordinary sensing performance. However, the simplest spray coating preparation method gives our sensor more potential for practical use, and the recyclable substrate makes it more environmentally friendly (Table S3). In summary, the HUBTPU combined with AgNWs successfully formed a kind of dual functional wearable device, which demonstrates favorable electrical heating capability and stable strain sensing functionality, manifesting a potential practical application value.

4. CONCLUSIONS

In summary, a facile one-pot method was developed to synthesize a series of hindered urea bond (HUB)-based polyurea elastomers using commercially available raw materials. HUBTPU-2 was selected to become the substrate for subsequent experiments due to the suitable mechanical behavior. Then, the reprocessability of HUBTPU-2 was investigated to meet the growing requirements of environmental protection. The results showed that the activation energy of as-synthesized HUBs was 109.66 kJ/mol and the cross-linked HUBTPU-2 turned into reprocessable under the conditions of 130 °C, 10 MPa, and 60 min. Moreover, the stress and strain at break remained approximately 80% compared to the original. Unsurprisingly, HUBTPU-2 demonstrated favorable adhesive properties to a diverse substrate, which enhanced the interface bonding between AgNWs.

The as-prepared HUBTPU electrodes demonstrated great durability compared to the PDMS electrodes, and the sheet resistance remained nearly unchanged after sonication, which could be attributed to the excellent interfacial adhesion between HUBTPU and AgNWs and the embedded structure. The HUBTPU electrodes showed a low sheet resistance of about 1 Ω/sq., capable of heating up to about 40−50 °C, which was suitable to warm the human body and then reached a maximum temperature of 115.6 °C when applying a voltage of 2.5 V. The strain sensing function was endowed by AgNWs, and as-prepared strain sensors successfully detected the movement signal of the human body. So far, dual functional wearable devices endowed with electrical heating and strain sensing functionalities based on reprocessable HUBTPUs and AgNWs were successfully demonstrated. This strategy could solve the interface adhesion problem between device polymers and rigid conductive materials.

■ ASSOCIATED CONTENT

Supporting Information

The Supporting Information is available free of charge at https://pubs.acs.org/doi/10.1021/acsami.2c11875.

Tables S1−S3: recipes of HUB-incorporated polyurea (HUBTPU) elastomers, comparison of various dynamic polymer networks synthesized using HUBs, and comparison of various strain sensors using AgNWs as a conductive component; Figures S1−S19: SEM image of the as-synthesized AgNWs, photographs of HUBTPU-2 soaked in various solvents before and after 48 h, gel contents of the HUBTPUs, FTIR spectra of monomers and HUBTPU-2, FTIR spectra of HUBTPUs, loading−unloading tensile curves of HUBTPU-2 and sequential cyclic tensile curves of HUBTPU-2, TG and DTG curves of HUBTPU-2, storage modulus and loss modulus of HUBTPU-2, DSC curve and tan δ of HUBTPUs, gel contents of HUBTPU-2 before and after reprocessing, temperature dependence of the thermal expansion curve of HUBTPU-2, FTIR spectra of HUBTPU-2 before and after reprocessing, gel contents of HUBTPU-2 before and after reprocessing, storage modulus of HUBTPU-2 before and after three times reprocessing, schematic demonstration of a hypothetical degradation mechanism of HUBTPU, DSC curve and tan δ of HUBTPU-2 after three times reprocessing, SEM images of PMDS electrodes before and after sonication, SEM images of the cross section and surface of liquid nitrogen brittle fractured HUBTPU electrode, photograph of the peeling text and the peeling strength of the HUBTPU and human skin, and response time of as-prepared strain sensors (PDF)

■ AUTHOR INFORMATION

Corresponding Author

Aimin Zhang − *State Key Laboratory of Polymer Materials Engineering, Polymer Research Institute of Sichuan University, Chendu 610065, China;* orcid.org/0000-0001-6518-200X; Email: zhangaimin@scu.edu.cn

Authors

Xingyuan Lu − *State Key Laboratory of Polymer Materials Engineering, Polymer Research Institute of Sichuan University, Chendu 610065, China*

Lun Zhang − *State Key Laboratory of Polymer Materials Engineering, Polymer Research Institute of Sichuan University, Chendu 610065, China*

Jihai Zhang − *State Key Laboratory of Polymer Materials Engineering, Polymer Research Institute of Sichuan University, Chendu 610065, China*

Chao Wang − *National Engineering Research Center for Synthesis of Novel Rubber and Plastic Materials, SINOPEC, Beijing Research Institute of Chemical Industry, Yanshan Branch, Beijing 102500, China*

Complete contact information is available at: https://pubs.acs.org/10.1021/acsami.2c11875

Notes

The authors declare no competing financial interest.

■ ACKNOWLEDGMENTS

X.L., L.Z., J.Z., C.W., and A.Z. received funding from the State Key Laboratory of Polymer Materials Engineering (grant no. sklpme2019-2-17). X.L., L.Z., J.Z., C.W., and A.Z. received funding from Putian City Regional Key Projects (grant no. 2020GJQ002). X.L., L.Z., J.Z., C.W., and A.Z. received funding from Huantai County Science and Technology Bureau (grant no. 20H1116).

https://doi.org/10.1021/acsami.2c11875
ACS Appl. Mater. Interfaces XXXX, XXX, XXX−XXX

REFERENCES

(1) Yu, L.; Yi, Y.; Yao, T.; Song, Y.; Chen, Y.; Li, Q.; Xia, Z.; Wei, N.; Tian, Z.; Nie, B.; Zhang, L.; Liu, Z.; Sun, J. All VN-Graphene Architecture Derived Self-Powered Wearable Sensors for Ultrasensitive Health Monitoring. *Nano Res.* **2019**, *12*, 331−338.

(2) Lin, H.; Tan, J.; Zhu, J.; Lin, S.; Zhao, Y.; Yu, W.; Hojaiji, H.; Wang, B.; Yang, S.; Cheng, X.; Wang, Z.; Tang, E.; Yeung, C.; Emaminejad, S. A Programmable Epidermal Microfluidic Valving System for Wearable Biofluid Management and Contextual Biomarker Analysis. *Nat. Commun.* **2020**, *11*, 4405.

(3) Liao, X.; Liao, Q.; Yan, X.; Liang, Q.; Si, H.; Li, M.; Wu, H.; Cao, S.; Zhang, Y. Flexible and Highly Sensitive Strain Sensors Fabricated by Pencil Drawn for Wearable Monitor. *Adv. Funct. Mater.* **2015**, *25*, 2395−2401.

(4) Cao, J.; Zhou, Z.; Song, Q.; Chen, K.; Su, G.; Zhou, T.; Zheng, Z.; Lu, C.; Zhang, X. Ultrarobust Ti3C2Tx MXene-Based Soft Actuators via Bamboo-Inspired Mesoscale Assembly of Hybrid Nanostructures. *ACS Nano* **2020**, *14*, 7055−7065.

(5) Cao, Y.; Tan, Y. J.; Li, S.; Lee, W. W.; Guo, H.; Cai, Y.; Wang, C.; Tee, B. C. K. Self-Healing Electronic Skins for Aquatic Environments. *Nat. Electron.* **2019**, *2*, 75−82.

(6) Cao, Y.; Morrissey, T. G.; Acome, E.; Allec, S. I.; Wong, B. M.; Keplinger, C.; Wang, C. A Transparent, Self-Healing, Highly Stretchable Ionic Conductor. *Adv. Mater.* **2017**, *29*, 1605099.

(7) Li, T.; Wang, Y.; Li, S.; Liu, X.; Sun, J. Mechanically Robust, Elastic, and Healable Ionogels for Highly Sensitive Ultra-Durable Ionic Skins. *Adv. Mater.* **2020**, *32*, No. e2002706.

(8) Zhang, P.; Guo, W.; Guo, Z. H.; Ma, Y.; Gao, L.; Cong, Z.; Zhao, X. J.; Qiao, L.; Pu, X.; Wang, Z. L. Dynamically Crosslinked Dry Ion-Conducting Elastomers for Soft Iontronics. *Adv. Mater.* **2021**, No. e2101396.

(9) Dang, C.; Wang, M.; Yu, J.; Chen, Y.; Zhou, S.; Feng, X.; Liu, D.; Qi, H. Transparent, Highly Stretchable, Rehealable, Sensing, and Fully Recyclable Ionic Conductors Fabricated by One-Step Polymerization Based on a Small Biological Molecule. *Adv. Funct. Mater.* **2019**, *29*, 1902467.

(10) Kai, H.; Suda, W.; Ogawa, Y.; Nagamine, K.; Nishizawa, M. Intrinsically Stretchable Electrochromic Display by a Composite Film of Poly(3,4-ethylenedioxythiophene) and Polyurethane. *ACS Appl. Mater. Interfaces* **2017**, *9*, 19513−19518.

(11) Li, H.; McRae, L.; Elezzabi, A. Y. Solution-Processed Interfacial PEDOT:PSS Assembly into Porous Tungsten Molybdenum Oxide Nanocomposite Films for Electrochromic Applications. *ACS Appl. Mater. Interfaces* **2018**, *10*, 10520−10527.

(12) Chen, W. H.; Li, F. W.; Liou, G. S. Novel Stretchable Ambipolar Electrochromic Devices Based on Highly Transparent AgNW/PDMS Hybrid Electrodes. *Adv. Opt. Mater.* **2019**, *7*, 1900632.

(13) Ahn, S.; Han, T. H.; Maleski, K.; Song, J.; Kim, Y. H.; Park, M. H.; Zhou, H.; Yoo, S.; Gogotsi, Y.; Lee, T. W. A 2D Titanium Carbide MXene Flexible Electrode for High-Efficiency Light-Emitting Diodes. *Adv. Mater.* **2020**, *32*, No. e2000919.

(14) Li, H.; Chen, J.; Chang, X.; Xu, Y.; Zhao, G.; Zhu, Y.; Li, Y. A Highly Stretchable Strain Sensor with Both an Ultralow Detection Limit and an Ultrawide Sensing Range. *J. Mater. Chem. A* **2021**, *9*, 1795−1802.

(15) Wang, R.; Jiang, N.; Su, J.; Yin, Q.; Zhang, Y.; Liu, Z.; Lin, H.; Moura, F. A.; Yuan, N.; Roth, S.; Rome, R. S.; Ovalle-Robles, R.; Inoue, K.; Yin, S.; Fang, S.; Wang, W.; Ding, J.; Shi, L.; Baughman, R. H.; Liu, Z. A Bi-Sheath Fiber Sensor for Giant Tensile and Torsional Displacements. *Adv. Funct. Mater.* **2017**, *27*, 1702134.

(16) Wang, R.; Liu, Z.; Wan, G.; Jia, T.; Zhang, C.; Wang, X.; Zhang, M.; Qian, D.; de Andrade, M. J.; Jiang, N.; Yin, S.; Zhang, R.; Feng, D.; Wang, W.; Zhang, H.; Chen, H.; Wang, Y.; Ovalle-Robles, R.; Inoue, K.; Lu, H.; Fang, S.; Baughman, R. H.; Liu, Z. Controllable Preparation of Ordered and Hierarchically Buckled Structures for Inflatable Tumor Ablation, Volumetric Strain Sensor, and Communication via Inflatable Antenna. *ACS Appl. Mater. Interfaces* **2019**, *11*, 10862−10873.

(17) Kang, D. H.; Cho, S.; Sung, S.; Kim, Y. R.; Lee, H.; Choe, A.; Yeom, J.; Kim, M. P.; Kim, J. C.; Noh, S. M.; Ko, H. Highly Transparent, Flexible, and Self-Healable Thermoacoustic Loudspeakers. *ACS Appl. Mater. Interfaces* **2020**, *12*, 53184−53192.

(18) Han, J.; Yang, J.; Gao, W.; Bai, H. Ice-Templated, Large-Area Silver Nanowire Pattern for Flexible Transparent Electrode. *Adv. Funct. Mater.* **2021**, 2010155.

(19) Deng, B.; Hsu, P. C.; Chen, G.; Chandrashekar, B. N.; Liao, L.; Ayitimuda, Z.; Wu, J.; Guo, Y.; Lin, L.; Zhou, Y.; Aisijiang, M.; Xie, Q.; Cui, Y.; Liu, Z.; Peng, H. Roll-to-Roll Encapsulation of Metal Nanowires between Graphene and Plastic Substrate for High-Performance Flexible Transparent Electrodes. *Nano Lett.* **2015**, *15*, 4206−4213.

(20) Park, S. B.; Han, J. W.; Kim, J. H.; Wibowo, A. F.; Prameswati, A.; Park, J.; Lee, J.; Moon, M. W.; Kim, M. S.; Kim, Y. H. Multifunctional Stretchable Organic−Inorganic Hybrid Electronics with Transparent Conductive Silver Nanowire/Biopolymer Hybrid Films. *Adv. Opt. Mater.* **2021**, 2002041.

(21) Dong, G. P.; Liu, S.; Pan, M. Q.; Zhou, G. F.; Liu, J. M.; Kempa, K.; Gao, J. W. Bioinspired High-Adhesion Metallic Networks as Flexible Transparent Conductors. *Adv. Mater. Technol.* **2019**, *4*, 1900056.

(22) Capelot, M.; Unterlass, M. M.; Tournilhac, F.; Leibler, L. Catalytic Control of the Vitrimer Glass Transition. *ACS Macro Lett.* **2012**, *1*, 789−792.

(23) Denissen, W.; Rivero, G.; Nicolay, R.; Leibler, L.; Winne, J. M.; Du Prez, F. E. Vinylogous Urethane Vitrimers. *Adv. Funct. Mater.* **2015**, *25*, 2451−2457.

(24) Chen, Y.; Tang, Z.; Liu, Y.; Wu, S.; Guo, B. Mechanically Robust, Self-Healable, and Reprocessable Elastomers Enabled by Dynamic Dual Cross-Links. *Macromolecules* **2019**, *52*, 3805−3812.

(25) Montarnal, D.; Capelot, M.; Tournilhac, F.; Leibler, L. Silica-Like Malleable Materials from Permanent Organic Networks. *Science* **2011**, *334*, 965−968.

(26) Pepels, M.; Filot, I.; Klumperman, B.; Goossens, H. Self-healing systems based on disulfide-thiol exchange reactions. *Polym. Chem.* **2013**, *4*, 4955−4965.

(27) Pei, Z.; Yang, Y.; Chen, Q.; Terentjev, E.; Wei, Y.; Ji, Y. Mouldable Liquid-Crystalline Elastomer Actuators with Exchangeable Covalent Bonds. *Nat. Mater.* **2014**, *13*, 36−41.

(28) Taynton, P.; Yu, K.; Shoemaker, R. K.; Jin, Y.; Qi, H.; Zhang, W. Heat- or Water-Driven Malleability in a Highly Recyclable Covalent Network Polymer. *Adv. Mater.* **2014**, *26*, 3938−3942.

(29) Trovatti, E.; Lacerda, T. M.; Carvalho, A. J. F.; Gandini, A. Recycling Tires? Reversible Crosslinking of Poly(butadiene). *Adv. Mater.* **2015**, *27*, 2242.

(30) Jia, Y.; Ying, H.; Zhang, Y.; He, H.; Cheng, J. Reconfigurable Poly(urea-urethane) Thermoset Based on Hindered Urea Bonds with Triple-Shape-Memory Performance. *Macromol. Chem. Phys.* **2019**, *220*, 1900148.

(31) Jams, I. B.; Windsor, F. M.; Poudevigne-Durance, T.; Ormerod, S. J.; Durance, I. Estimating the Size Distribution of Plastics Ingested by Animals. *Nat. Commun.* **2020**, *11*, 1594.

(32) Jiang, L.; Lei, Y.; Xiao, Y.; Fu, X.; Kong, W.; Wang, Y.; Lei, J. Mechanically Robust, Exceptionally Recyclable and Shape Memory Cross-Linked Network Based on Reversible Dynamic Urea Bonds. *J. Mater. Chem. A* **2020**, *8*, 22369−22378.

(33) Fang, Z.; Zheng, N.; Zhao, Q.; Xie, T. Healable, Reconfigurable, Reprocessable Thermoset Shape Memory Polymer with Highly Tunable Topological Rearrangement Kinetics. *ACS Appl. Mater. Interfaces* **2017**, *9*, 22077−22082.

(34) Zhang, Y.; Ying, H.; Hart, K. R.; Wu, Y.; Hsu, A. J.; Coppola, A. M.; Kim, T. A.; Yang, K.; Sottos, N. R.; White, S. R.; Cheng, J. Malleable and Recyclable Poly(urea-urethane) Thermosets bearing Hindered Urea Bonds. *Adv. Mater.* **2016**, *28*, 7646−7651.

(35) Zhou, Z.; Zeng, Y.; Yu, C.; Chen, H.; Zhang, F. Mechanically Robust, Intrinsically Self-Healing Crosslinked Polymer Enabled by Dynamic Urea Bond Exchange Reaction. *ACS Appl. Mater. Interfaces* **2020**, *29*, 115041.

https://doi.org/10.1021/acsami.2c11875
ACS Appl. Mater. Interfaces XXXX, XXX, XXX−XXX

(36) Qin, B.; Zhang, S.; Sun, P.; Tang, B.; Yin, Z.; Cao, X.; Chen, Q.; Xu, J. F.; Zhang, X. Tough and Multi-Recyclable Cross-Linked Supramolecular Polyureas via Incorporating Noncovalent Bonds into Main-Chains. *Adv. Mater.* **2020**, *32*, No. e2000096.
(37) Ding, H.; Zhao, B.; Mei, H.; Li, L.; Zheng, S. Transformation of Commodity Poly(hydroxyether of bisphenol A) into Vitrimers via Post Crosslinking with Hindered Urea Bonds. *Chin. J. Polym. Sci.* **2020**, *38*, 915−920.
(38) Jiang, L.; Liu, Z.; Lei, Y.; Yuan, Y.; Wu, B.; Lei, J. Sustainable Thermosetting Polyurea Vitrimers Based on a Catalyst-Free Process with Reprocessability, Permanent Shape Reconfiguration and Self-Healing Performance. *ACS Appl. Polym. Mater.* **2019**, *1*, 3261−3268.
(39) Wang, Z.; Yang, M.; Wang, X.; Fei, G.; Zheng, Z.; Xia, H. NIR Driven Fast Macro-Damage Repair and Shear-Free Reprocessing of Thermoset Elastomers via Dynamic Covalent Urea Bonds. *J. Mater. Chem. A* **2020**, *8*, 25047−25052.
(40) Scott, T. F.; Schneider, A. D.; Cook, W. D.; Bowman, C. N. Photoinduced Plasticity in Cross-Linked Polymers. *Science* **2005**, *308*, 1615−1617.
(41) Rekondo, A.; Martin, R.; de Luzuriaga, A. r.; Cabanero, G.; Grande, H. J.; Odriozola, I. Catalyst-Free Room-Temperature Self-Healing Elastomers Based on Aromatic Disulfide Metathesis. *Mater. Horiz.* **2014**, *1*, 237−240.
(42) Pickering, S. J. Recycling Technologies for Thermoset Composite Materials - Current Status. *Composites,Part A* **2006**, *37*, 1206−1215.
(43) Liu, S.; Chen, S.; Shi, W.; Peng, Z.; Luo, K.; Xing, S.; Li, J.; Liu, Z.; Liu, L. Self-Healing, Robust, and Stretchable Electrode by Direct Printing on Dynamic Polyurea Surface at Slightly Elevated Temperature. *Adv. Funct. Mater.* **2021**, *31*, 2102225.
(44) Yang, C.; Gu, H.; Lin, W.; Yuen, M. M.; Wong, C. P.; Xiong, M.; Gao, B. Silver Nanowires: From Scalable Synthesis to Recyclable Foldable Electronics. *Adv. Mater.* **2011**, *23*, 3052−3056.
(45) Zhang, L.; Liu, Z.; Wu, X.; Guan, Q.; Chen, S.; Sun, L.; Guo, Y.; Wang, S.; Song, J.; Jeffries, E. M.; He, C.; Qing, F.-L.; Bao, X.; You, Z. A Highly Efficient Self-Healing Elastomer with Unprecedented Mechanical Properties. *Adv. Mater.* **2019**, *31*, e1901402.
(46) Fu, D.; Pu, W.; Wang, Z.; Lu, X.; Sun, S.; Yu, C.; Xia, H. A Facile Dynamic Crosslinked Healable Poly(oxime-urethane) Elastomer with High Elastic Recovery and Recyclability. *J. Mater. Chem. A* **2018**, *6*, 18154−18164.
(47) Wu, B.; Lei, Y.; Xiao, Y.; Wang, Y.; Yuan, Y.; Jiang, L.; Zhang, X.; Lei, J. A Bio-Inspired and Biomass-Derived Healable Photochromic Material Induced by Hierarchical Structural Design. *Macromol. Mater. Eng.* **2020**, *305*, 1900539.
(48) Zhang, Q.; Shi, C.-Y.; Qu, D.-H.; Long, Y.-T.; Feringa, B. L.; Tian, H. Exploring a Naturally Tailored Small Molecule for Stretchable, Self-Healing, and Adhesive Supramolecular Polymers. *Sci. Adv.* **2018**, *4*, eaat8192.
(49) Yu, X.; Wang, Y.; Zhang, H.; Fan, X.; Liu, T. Ultrastretchable and Stable Conductive Elastomer Based on Micro-Ionicgel for Wide-Working-Range Sensors. *ACS Appl. Mater. Interfaces* **2021**, 53091.
(50) Cai, K.; Ying, H.; Cheng, J. Dynamic Ureas with Fast and pH-Independent Hydrolytic Kinetics. *Chemistry* **2018**, *24*, 7345−7348.
(51) Ying, H.; Cheng, J. Hydrolyzable Polyureas Bearing Hindered Urea Bonds. *J. Am. Chem. Soc.* **2014**, *136*, 16974−16977.
(52) Patel, T.; Kim, M. P.; Park, J.; Lee, T. H.; Nellepalli, P.; Noh, S. M.; Jung, H. W.; Ko, H.; Oh, J. K. Self-Healable Reprocessable Triboelectric Nanogenerators Fabricated with Vitrimeric Poly-(hindered Urea) Networks. *ACS Nano* **2020**, *14*, 11442−11451.
(53) Zhang, J.; Zhang, C.; Song, F.; Shang, Q.; Hu, Y.; Jia, P.; Liu, C.; Hu, L.; Zhu, G.; Huang, J.; Zhou, Y. Castor-Oil-Based, Robust, Self-Healing, Shape Memory, and Reprocessable Polymers Enabled by Dynamic Hindered Urea Bonds and Hydrogen Bonds. *Chem. Eng. J.* **2022**, *429*, 131848.
(54) Ying, H.; Zhang, Y.; Cheng, J. Dynamic Urea Bond for the Design of Reversible and Self-Healing Polymers. *Nat. Commun.* **2014**, *5*, 1.

https://doi.org/10.1021/acsami.2c11875
ACS Appl. Mater. Interfaces XXXX, XXX, XXX−XXX